Electronic Supplementary Material (ESI) for Dalton Transactions.
This journal is © The Royal Society of Chemistry 2021

Supporting Information

Spin and Valence Isomerism in Cyanide-Bridged $\{Fe^{III}_2M^{II}\}$ (M = Fe, Co) Clusters

Xin-Hua Zhao,[a] Dong Shao,[a] Jia-Tao Chen,[a] Min Liu,[b] Tao Li,[a] Jiong Yang,[a] and Yuan-Zhu Zhang*[a]

[a] *Department of Chemistry, Southern University of Science and Technology, Shenzhen, 518055, P. R. China.*

[b] *College of Nuclear Science and Technology, University of South China, Hengyang, 421001, P. R. China.*

Table S1 Selected bond lengths [Å] and bond angles [°] for **1**.

	100 K	290 K
Fe1-N1	1.994(4)	2.153(4)
Fe1-N2	2.059(4)	2.219(4)
Fe1-N3	1.934(4)	2.059(4)
Fe2-N6	2.009(4)	2.000(4)
Fe2-N8	1.972(4)	1.978(4)
Fe2-N10	2.014(4)	2.006(4)
Fe2-C14	1.918(5)	1.897(5)
Fe2-C15	1.936(5)	1.927(5)
Fe2-C16	1.923(5)	1.924(6)
Fe1-Fe1	4.994(1)	5.093(1)
N1-Fe1-N1A	178.0(2)	172.1(2)
N1-Fe1-N2A	97.9(2)	97.7(2)
N1-Fe1-N2	80.6(2)	76.3(2)
N2-Fe1-N2A	85.9(2)	81.8(2)
N3A-Fe1-N1	92.7(2)	94.1(2)
N3-Fe1-N1	88.7(2)	91.4(2)
N3A-Fe1-N2	172.8(2)	168.4(2)
N3-Fe1-N2	92.5(2)	93.4(2)
N3-Fe1-N3A	90.0(2)	93.3(2)
C14-N3-Fe1	177.5(4)	176.9(4)
N3-C14-Fe2	171.4(4)	173.1(5)
Fe2-Fe1-Fe2A	92.7(1)	94.1(1)

A -x+1,y,-z+1/2

Table S2 The hydrogen bonds in **1** at 100 K.

D-H···A	D-H [Å]	H···A [Å]	D···A [Å]	∠D-H···A [°]
O1-H1B ···N4	0.84	2.56	3.07(2)	120
O2-H2A ···N5	0.87	2.21	2.99(3)	149
O2-H2B ···O3	0.87	1.89	2.36(4)	112
O3-H3A ···O2	0.87	1.60	2.36(4)	144
O4-H4A ···N5	0.87	2.51	3.16(3)	132

Table S3 Selected bond lengths [Å] and bond angles [°] for **2**.

	100 K	300 K
Co1-N1	2.024(6)	2.115(4)
Co1-N2	2.028(6)	2.141(4)
Co1-N3	1.966(5)	2.036(4)
Fe1-N6	1.982(5)	1.973(3)
Fe1-N8	2.020(5)	2.015(3)
Fe1-N10	2.029(5)	2.027(4)
Fe1-C14	1.913(7)	1.904(5)
Fe1-C15	1.923(7)	1.929(5)
Fe1-C16	1.935(6)	1.935(5)
Fe1-Co1	5.015(1)	5.076(1)
N1-Co1-N1A	176.2(3)	174.1(2)
N1-Co1-N2A	98.5(3)	99.3(2)
N1-Co1-N2	78.6(3)	76.2(2)
N1-Co1-N3	93.4(2)	94.3(2)
N1A-Co1-N3	89.2(2)	89.8(2)
N2-Co1-N3	171.0(3)	168.6(2)
N2A-Co1-N3	93.3(2)	93.6(2)
N2-Co1-N2A	83.9(4)	82.0(2)
N3-Co1-N3A	90.7(3)	92.7(2)
C14-N3-Co1	177.2(5)	176.7(3)
N3-C14-Fe1	172.1(6)	172.8(4)
Fe1-Co1-Fe1A	92.8(2)	94.0(1)

A -x+1,y,-z+3/2

Table S4 The hydrogen bonds in **2** at 100 K.

D-H···A	D-H [Å]	H···A [Å]	D···A [Å]	∠D-H···A [°]
O1-H1B ···N4	0.84	2.14	2.82(2)	138
O4-H4A ···O5	0.87	1.96	2.77(4)	152
O5-H5B ···N4	0.87	2.45	3.05(2)	127

Table S5 CV data of complex **2**.

	E_{pa} [V]	E_{pc} [V]	$E_{1/2}$ [V]	ΔE [V]
$[Fe^{II}_2Co^{II}]^{2-}/[Fe^{III}Fe^{II}Co^{II}]^{-}$	-0.551	-0.795	-0.673	
$[Fe^{III}Fe^{II}Co^{II}]^{-}/[Fe^{III}_2Co^{II}]$	-0.063	-0.317	-0.190	0.538
$[Fe^{III}_2Co^{II}]/[Fe^{III}_2Co^{II}]^{+}$	0.531	0.165	0.348	

Table S6 Thermal dynamic parameters derived from the fitting of $\chi_M T$ vs. T plots for **1** and **2**.

Compound	ΔH (kJ mol^{-1})	ΔS (J mol^{-1} K^{-1})	$T_{1/2}$ (K)	Γ (kJ mol^{-1})
1	21.87	87.46	250	0.42
2	15.42	84.49	182	-0.84

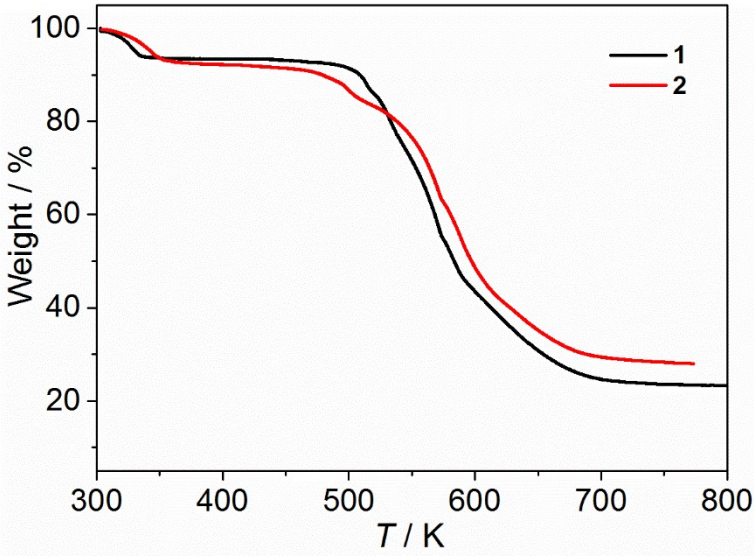

Fig. S1 TGA curves of **1** and **2** at a rate of 10 K/min under an argon atmosphere.

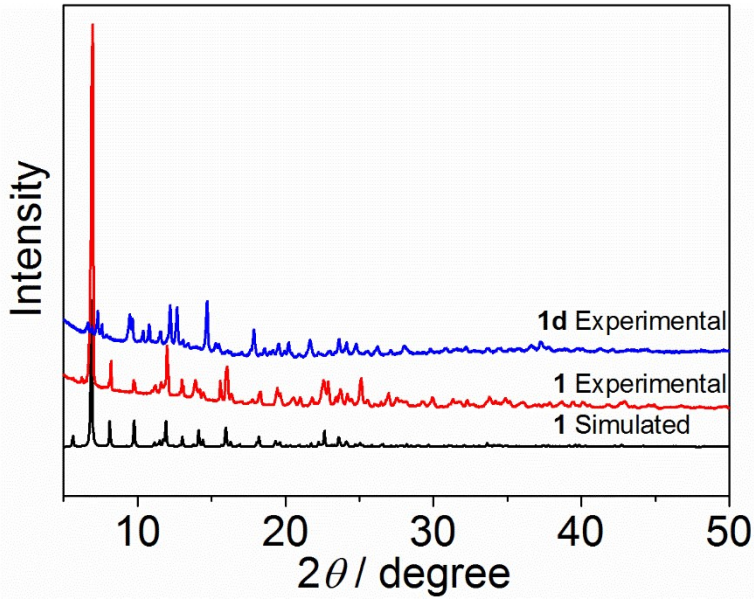

Fig. S2 The experimental and simulated PXRD patterns of **1** and **1d**.

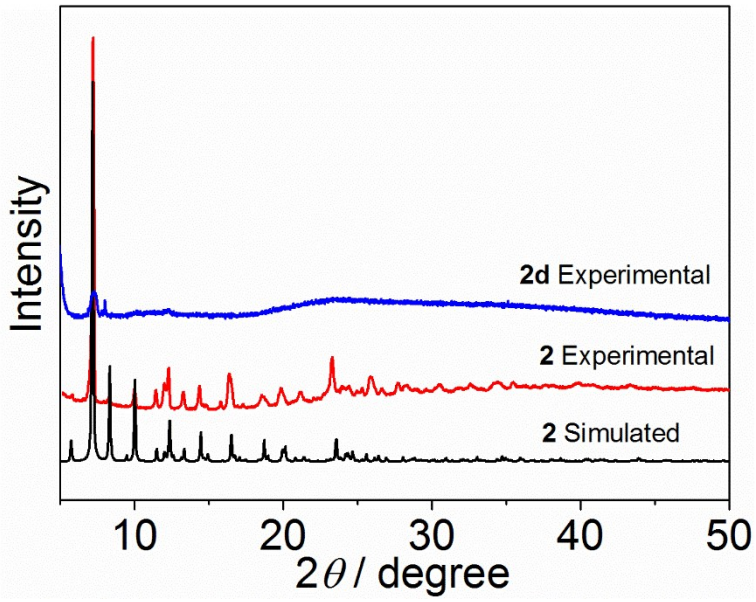

Fig. S3 The experimental and simulated PXRD patterns of **2** and **2d**.

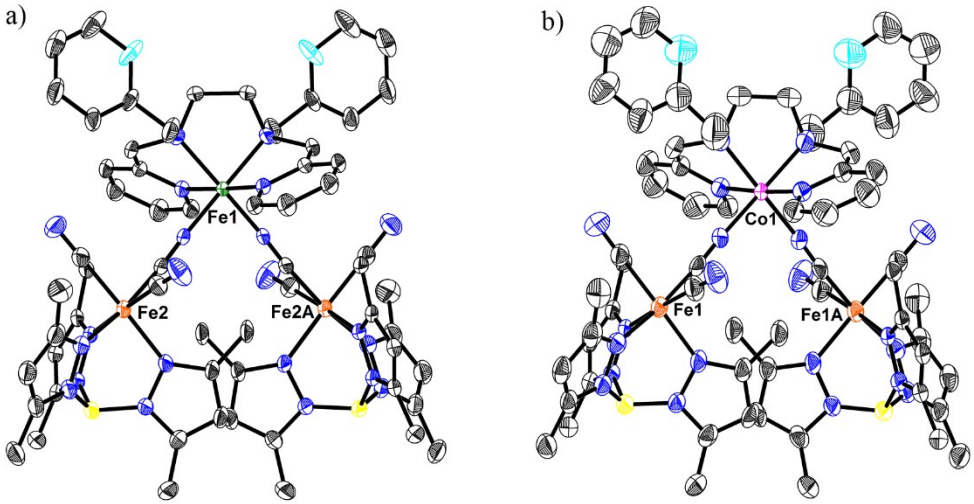

Fig. S4 ORTEP drawing of a) [{Tp*Fe(CN)$_3$}$_2$Fe(bztpen)}] for **1** and b) [{Tp*Fe(CN)$_3$}$_2$Co(bztpen)}] for **2**. Ellipsoids enclose 50% probability. The hydrogen atoms and solvent molecules have been omitted for clarity.

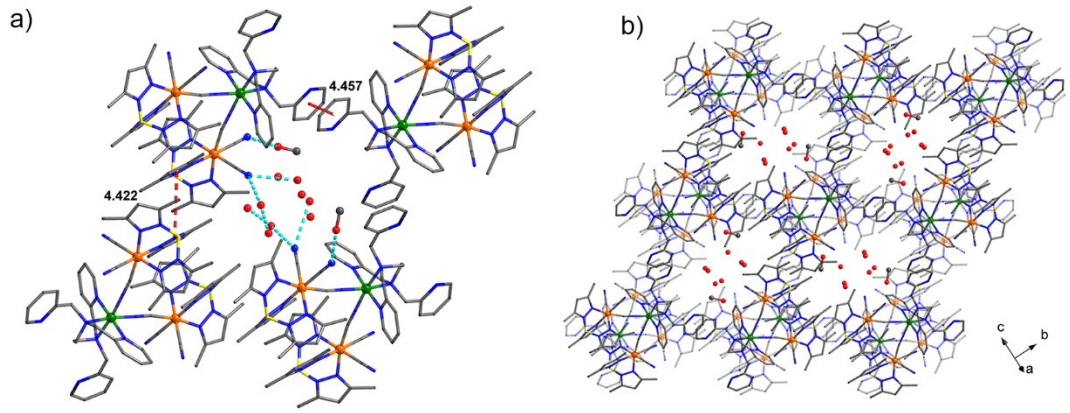

Fig. S5 a) The intermolecular interactions between neighbouring {Fe_2Fe} and the lattice solvents for **1**, the turquiose and red dashed lines represent the hydrogen bonds and the center-center distances of neighboring pyridyl or pyrazolyl rings, respectively. b) The crystal packing of **1**.

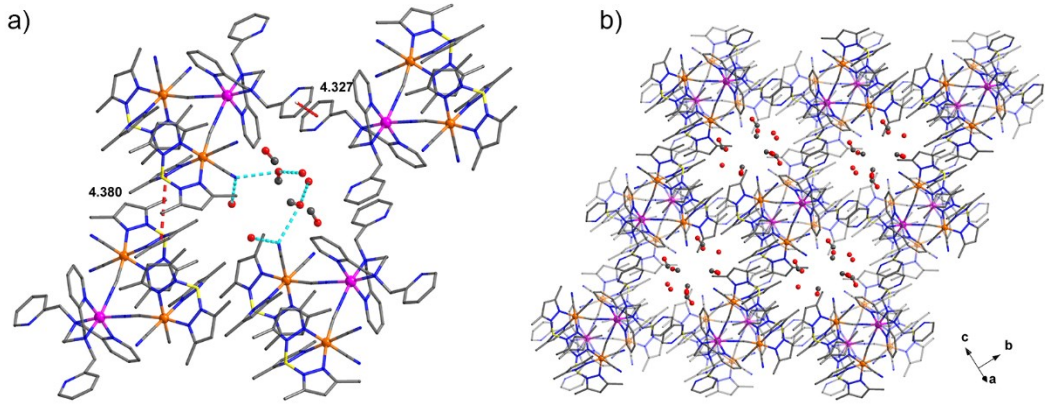

Fig. S6 a) The intermolecular interactions between neighbouring {Fe_2Co} and the lattice solvents for **2**, the turquiose and red dashed lines represent the hydrogen bonds and the centroid-centroid distances of neighboring pyridyl or pyrazolyl rings, respectively. b) The crystal packing of **2**.

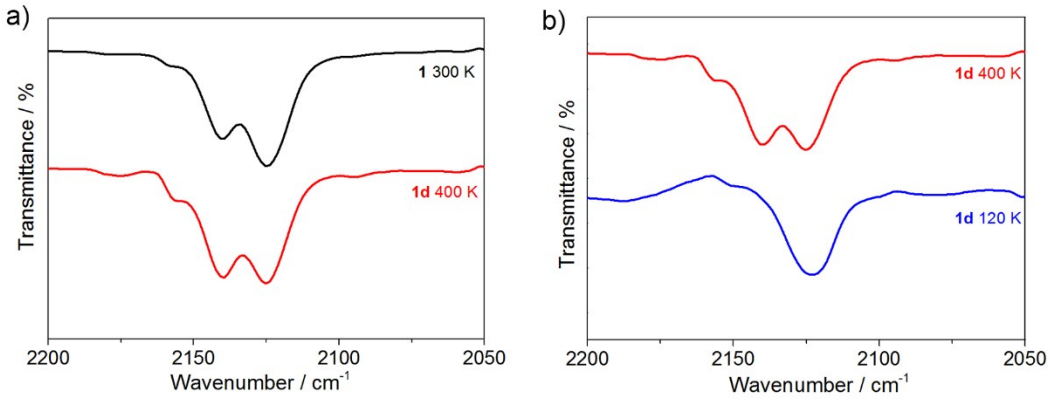

Fig. S7 Temperature-dependent IR spectra of **1** and **1d**.

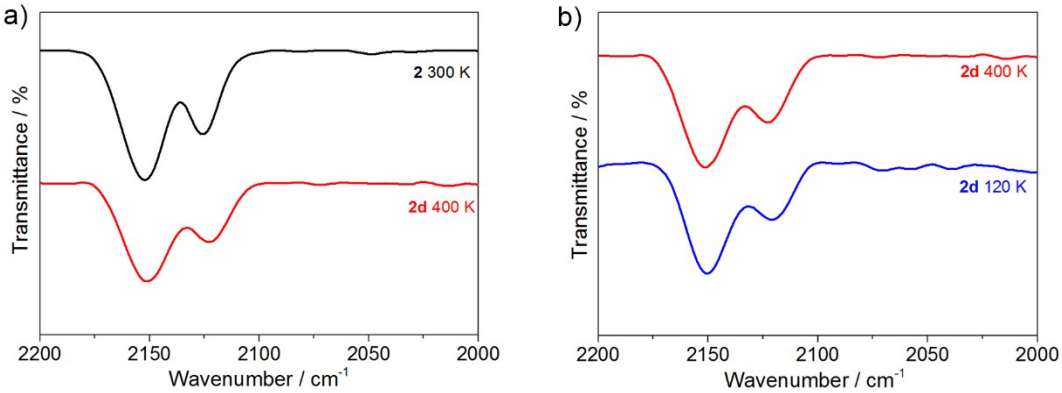

Fig. S8 Temperature-dependent IR spectra of **2** and **2d**.

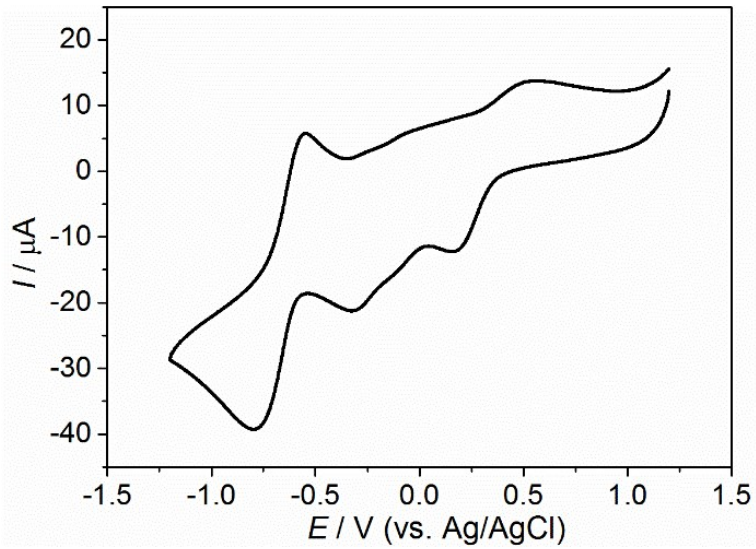

Fig. S9 Cyclic voltammogram of **2** in 0.1M $(nBu_4)PF_6$ in CH_2Cl_2.

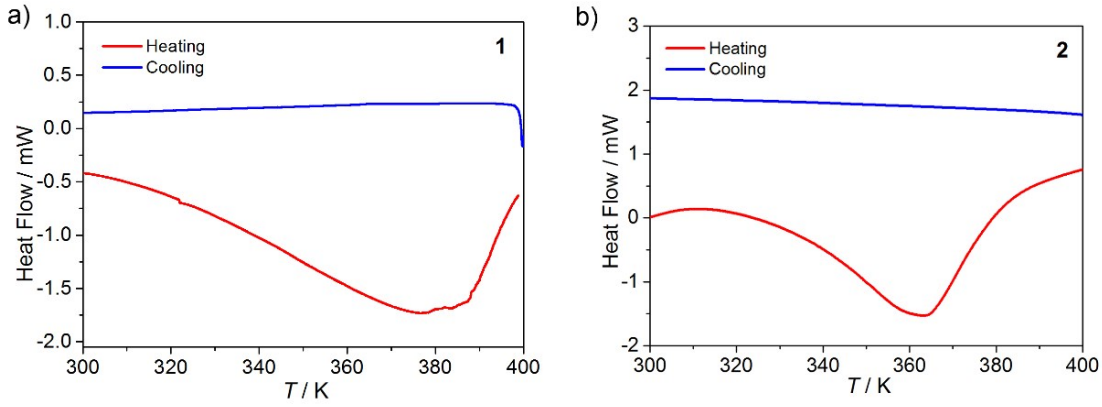

Fig. S10 DSC curves of a) **1** and b) **2**.

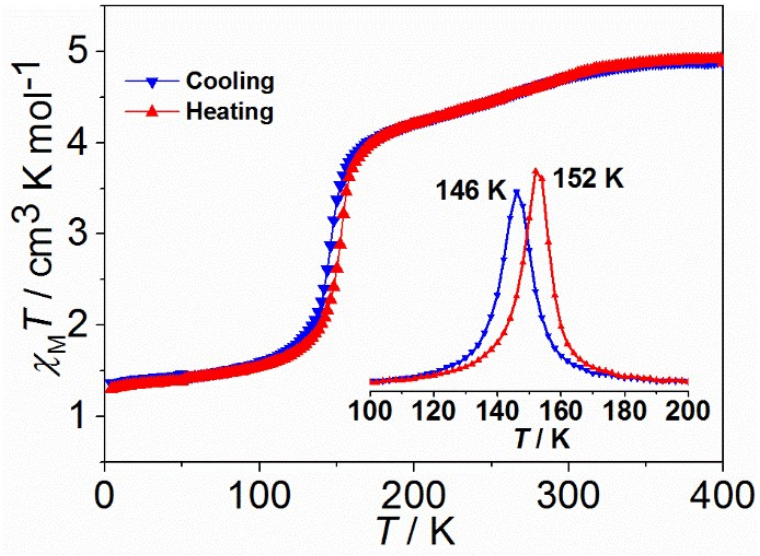

Fig. S11 Temperature dependent $\chi_M T$ plots of **1d** under a sweeping rate of 2 K/min, insert: The d($\chi_M T$)/dT vs T plots used to determine the $T_{1/2}$ values.

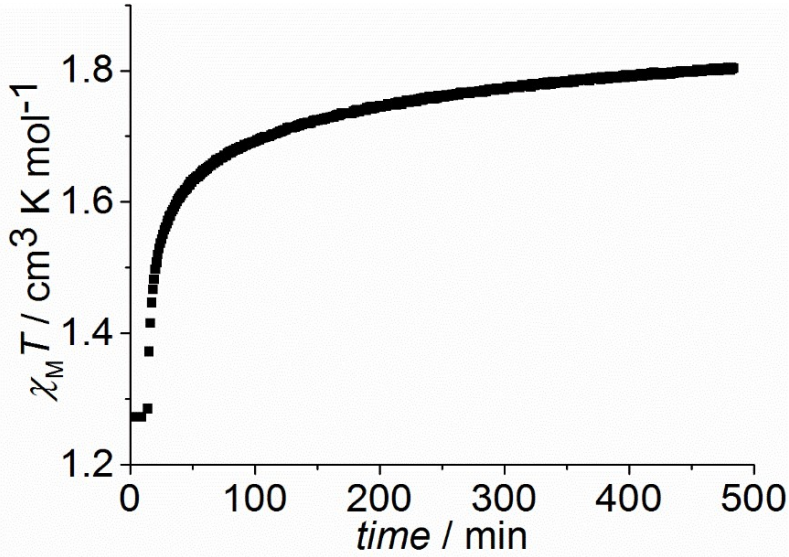

Fig. S12 $\chi_M T$ vs time plot of **2** irradiated at 808 nm at 20 K.

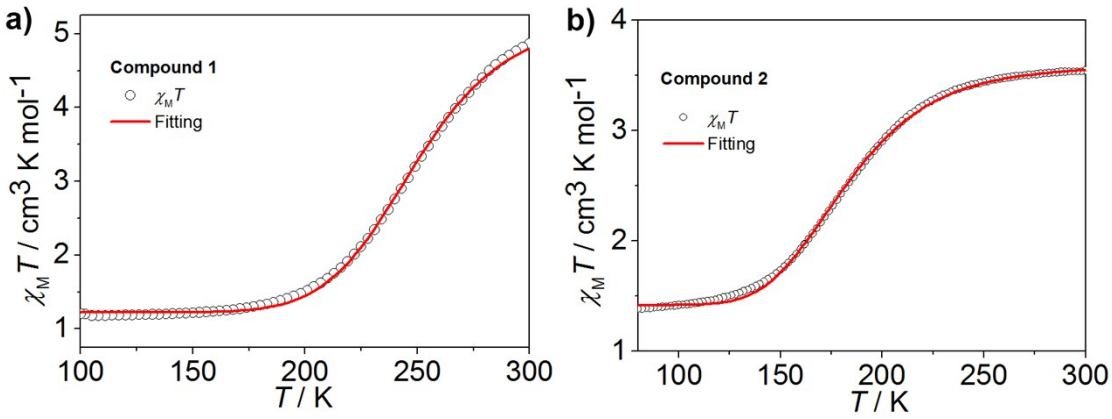

Fig. S13 Temperature-dependent $\chi_M T$ plots for a) **1** and b) **2** in the cooling mode, the red lines represent the best fitting using the Slichder-Drickamer model.